Analyst

PAPER

View Article Online
View Journal | View Issue

Cite this: *Analyst*, 2024, **149**, 1527

Multiplex detection of the big five carbapenemase genes using solid-phase recombinase polymerase amplification†‡

Christopher L. Johnson, §[a] Matthew A. Setterfield,§[a] Waleed A. Hassanain, [b] Anil Wipat,[c] Matthew Pocock,[c] Karen Faulds, [b] Duncan Graham [b] and Neil Keegan*[a]

Five carbapenemase enzymes, coined the 'big five', have been identified as the biggest threat to world-wide antibiotic resistance based on their broad substrate affinity and global prevalence. Here we show the development of a molecular detection method for the gene sequences from the five carbapenemases utilising the isothermal amplification method of recombinase polymerase amplification (RPA). We demonstrate the successful detection of each of the big five carbapenemase genes with femtomolar detection limits using a spatially separated multiplex amplification strategy. The approach uses tailed oligonucleotides for hybridisation, reducing the complexity and cost of the assay compared to classical RPA detection strategies. The reporter probe, horseradish peroxidase, generates the measureable output on a benchtop microplate reader, but more notably, our study leverages the power of a portable Raman spectrometer, enabling up to a 19-fold enhancement in the limit of detection. Significantly, the development approach employed a solid-phase RPA format, wherein the forward primers targeting each of the five carbapenemase genes are immobilised to a streptavidin-coated microplate. The adoption of this solid-phase methodology is pivotal for achieving a successful developmental pathway when employing this streamlined approach. The assay takes 2 hours until result, including a 40 minutes RPA amplification step at 37 °C. This is the first example of using solid-phase RPA for the detection of the big five and represents a milestone towards the developments of an automated point-of-care diagnostic for the big five using RPA.

Received 10th October 2023,
Accepted 13th January 2024

DOI: 10.1039/d3an01747h

rsc.li/analyst

Introduction

Carbapenemase-producing Gram negative organisms

Carbapenemase-producing Gram negative organisms (CPO) are a group of Gram-negative bacteria that are resistant to carbapenem antibiotics and most other beta-lactams.[1] CPO include carbapenemase-producing Enterobacteriacae (CPE), carbapenem-resistant *Acinetobacter baumannii*, and carbapenem-resistant *Pseudomonas aeruginosa.*[2] CPO pose a major threat to public health due to their ability to evade treatment with one of the most important classes of antibiotics, the carbapenems.

Carbapenems, considered as last resort antibiotics, are a class of broad-spectrum antibiotics that are highly effective against a wide range of bacteria, including multidrug-resistant strains.[3] However, over time, bacteria have developed various mechanisms to resist the action of carbapenems, leading to the emergence of carbapenem-resistant bacteria.[4] By far the most prevalent mechanism of carbapenem resistance in Gram-negative bacteria is the production of carbapenemase enzymes.[5] Carbapenemases are beta-lactamases that have the ability to hydrolyse carbapenem antibiotics as well as other beta-lactams, rendering them ineffective and causing antibiotic resistance.[6]

Carbapenemases can be divided into four classes, A, B, C, and D based on their molecular and mechanistic properties.[7] Enzymes residing in classes A, C, and D all utilise an active site serine to hydrolyse the beta-lactam ring.[8] The inactivation of beta-lactams by class B enzymes is zinc-mediated, as such this class are designated metallo-beta-lactamases (MBLs).[9] The emergence of carbapenemase-producing bacteria, particularly

[a]*Diagnostic and Therapeutic Technologies, Translational and Clinical Research Institute, Newcastle University, Newcastle-Upon-Tyne, UK.*
E-mail: neil.keegan@ncl.ac.uk
[b]*Department of Pure and Applied Chemistry, Technology and Innovation Centre, University of Strathclyde, Glasgow, UK*
[c]*ICOS, School of Computing, Urban Sciences Building, Newcastle University, Newcastle-Upon-Tyne, UK*

† For all raw data files see **https://doi.org/10.25405/data.ncl.24199476.v2**.

‡ Electronic supplementary information (ESI) available. See DOI: **https://doi.org/10.1039/d3an01747h**

§ These authors contributed equally towards this work.

those harbouring the genes bla_{KPC} (class A), $bla_{OXA\text{-}48\text{-like}}$ (class D), bla_{VIM} (class B), bla_{NDM} (class B), and bla_{IMP} (class B) – from herein referred to as the big five carbapenemase genes – has complicated the management of bacterial infections and underscored the urgency of developing new strategies to control the spread of antibiotic resistance.

Advances in diagnostic methods for carbapenemase detection

The GeneXpert Carba-R test is a rapid molecular diagnostic assay for the detection of CPO in clinical specimens. The test uses multiplex real-time polymerase chain reaction (qPCR) to simultaneously amplify and detect target DNA sequences from the big five carbapenemase genes. The ability to detect multiple nucleic acid signatures simultaneously – multiplexed detection – further reduces the time and cost of screening and is particularly important for screening resistance mechanisms which are inherently heterogeneous. Ensuring that the primer pairs used in the qPCR do not interact during amplification and produce reliable, sensitive, and specific assays is not a trivial task. However, once the system is optimised and the conditions established the throughput of the system is increased considerably. The test is performed on the GeneXpert system, a fully automated platform that can deliver results in less than 1 h.[10,11] The system combines sample preparation, amplification and detection in a single cartridge, streamlining the process and minimising the risk of contamination. Another automated qPCR system which can screen for the big five is the BD MAX check-points CPO assay. A recent comparison of the BD MAX check-points CPO assay with Cepheid's Xpert Carba-R assay for the detection of CPO directly from rectal swabs found the Carba-R test was superior, although the overall performance of the BD MAX check-points CPO assay was excellent with accuracy, sensitivity, specificity, and NPV higher than 95%.[12] These cartridge based qPCR systems remove lab assay dependencies regarding highly skilled/trained personnel to perform and interpret the test. However, the instruments which house and run the microfluidic cartridges, and the individual test cartridges themselves are very expensive. In addition, mains electricity supplies and cold storage chains still need to be considered. Although these dependencies are not a major obstacle for developed countries, they are a huge barrier to implementation in low to middle income countries with a limited health infrastructure. The potential to translate PCR and amplification methodologies to point-of-care (PoC) settings has only partially been unlocked by the current miniaturised self-contained microfluidic lab-on-a-chip devices which integrate the fundamental steps of target detection.[13]

Recombinase polymerase amplification

The isothermal amplification method recombinase polymerase amplification (RPA) operates between 25 °C and 42 °C and has been shown to operate using body heat alone.[14,15] RPA has been extensively reviewed and is an effective PoC diagnostic technique due to its rapid and sensitive nature.[16,17] The proteins used in RPA are central components of *in vivo* processes required for cellular DNA synthesis, recombination, and repair.[18] RPA relies on three core proteins from T4 bacteriophage in combination with a strand displacing polymerase from *Bacillus subtilis* (*Bsu* polymerase) (Fig. S1‡). Magnesium serves as an indispensable cofactor for DNA polymerases, and consequently, due to the fact that RPA can work at these lower temperatures, the manufacturer of RPA kits recommends adding it at the last step of sample preparation in order to initiate amplification.[19]

Multiplex DNA detection is important for molecular diagnostics as it allows simultaneous identification and analysis of multiple targets, enabling a more efficient and comprehensive assessment of complex diseases or conditions in a single assay, thereby saving time, resources, and providing valuable insights for accurate patient management. Multiplex reactions can undertake various different strategies in order to successfully achieve multiplexed detection. Here we highlight the main variations for clarity. Single-tube multiplex assays involve the amplification and detection of two or more targets in the same reaction space. Spatially separated multiplex assays by comparison keep each of the reactions in discreet reaction spaces during amplification prior to detection. Single-tube multiplex assays generally offer advantages in terms of reduced reaction space and sample volume. However, these benefits come with the trade-off of an increased risk of non-specific interactions caused by the presence of multiple oligonucleotides required for the multiplex. Conversely, conducting a spatially separated multiplex mitigates the potential for non-specific interactions among the oligonucleotides in the sample, but necessitates a more complex reaction space, such as a microfluidic and larger sample volumes.[17]

RPA does have limitations such as the production of unexpected products due to the formation of primer-dimers, especially when the target DNA is present at low concentration.[20] Even so, the vast majority of research uses solution-phase RPA with primers that are free to diffuse for optimal reaction kinetics, nevertheless solid-phase RPA has also been employed to a overcome some of solution-phase RPA's limitations.[16] In solid-phase RPA one of the primers is immobilised on a solid support thereby limiting the availability of one of the two primers in solution. As the diffusion of one of the primers is impeded the amplification kinetics are reduced in solid-phase RPA compared to solution-phase.[16] However, this is balanced with the major advantage that it minimises the non-specific formation of primer-dimers which can be problematic in solution-phase RPA.[21] In addition, solid-phase amplification methods and the spatial resolution they provide makes them highly adaptable to multiplexed amplification while also providing the possibility to couple with diverse detection techniques.[22]

RPA detection employs various detection strategies including fluorescent probes, electrochemical detection and lateral flow strips.[17] In this research strategy the RPA amplification is coupled with resonance Raman spectroscopy (RRS) detection. Raman spectroscopy is a highly selective vibrational technique, which can characterise multiple compounds in a single solu-

tion based on their unique, sharp and well-resolved Raman peaks within complex spectra, and does so in real-time providing the potential for multiplexed analysis as a fingerprint technique.[23] To improve the sensitivity of Raman signal scattering, the excitation frequency can be tuned to be close to, or into resonance with, an electronic excited state of the molecule, namely RRS, which results in signal enhancements of up to 10^6 over normal Raman scattering.[24] Previous work has shown how effective RRS can be in the detection of target DNA, providing a more sensitive method of analysis than colorimetric techniques.[16] Moreover, recent advances in Raman spectrometers that can transfer the Raman readout from bench-top centralised laboratories to user-friendly and cost-effective portable readers suits the ultimate aim of developing of PoC scenario tests.[25]

Here we present the development of a pentaplex spatially separated solid-phase RPA assay for the detection of the big five carbapenemase genes. This represents a proof of principle that RPA detection of the big five, that relies solely on DNA–DNA hybridisation events to replace the need for multiple antibody and DNA tags, can be achieved using a resonance Raman portable reader. Calibration curves were generated successfully for each of the big five with femtomolar (fM) limits of detection (LOD) using a benchtop microplate reader. Additionally, the LOD could be improved up to 19-fold to achieve low fM detection by using a portable Raman spectrometer as an alternative readout of the solid-phase RPA reactions.

Experimental section

Solid-phase RPA combined with enzyme-linked oligonucleotide assay analysis

RPA was carried out using streptavidin-coated microplates as the solid-phase. The microplates were washed three times with phosphate buffered saline with $0.05\%_{(v/v)}$ tween-20 (PBSt) before functionalising overnight at 4 °C with 13.25 pmol of forward primer in 50 μL of phosphate buffered saline (PBS). Forward primers for the big five are each modified with a 5′-biotin-tetraethylene glycol spacer (5′-biotin-TEG), the biotin moiety being used for capture using the streptavidin coated microplate whilst the TEG acts as a spacer group. RPA liquid basic kits (TwistDX) were used for the assays and the master mix was made as per the manufacturer's instructions. Briefly, per reaction, 25 μL of 2× reaction buffer, 3.6 μL of 25 mM dNTP mix, 5 μL of 10× basic E-mix, 2.4 μL of 10 μM reverse primer, 4 μL of dH_2O, 2.5 μL of 20× core reaction mix and 2.5 μL of magnesium acetate were used. An RPA mastermix was prepared accordingly based on the above single reaction quantities up to the point of magnesium acetate addition. Meanwhile the functionalised microplate containing primers for the big five was washed three times with 200 μL of PBSt before adding 5 μL of either template for sample reactions or 5 μL of H_2O for no template control (NTC) reactions. Magnesium acetate (2.5 μl) was then added to the mastermix which was vortexed for 60 s prior to adding 45 μL of mastermix to either sample or NTC wells. The microplate was then covered with a plate seal and placed on a plate shaker (240 rpm, 37 °C) and the RPA reaction was allowed to proceed for 40 min. To carry out the enzyme-linked oligonucleotide assay (ELONA) the microplate was removed from the 37 °C oven and wells were washed three times with 200 μL of PBSt. Reporter probe (25 nM) in 4× SSC was then added to each of the wells before shaking at 240 rpm for 30 min to allow DNA–DNA hybridisation to occur. The microplate was then washed three times using PBSt before two washes using PBS. Finally, 100 μL of TMB peroxidase substrate (KPL SureBlue Seracare) was added to the wells and the absorbance was measured at 630 nm using a benchtop microplate reader (Tecan infinite M200).

Resonance Raman spectroscopy

RPA was carried out as per solid-phase RPA and ELONA analysis except 350 μl of TMB was added at the final step. For instrumentation see ESI.‡

For additional experimental details, please refer to the ESI.‡

Results and discussion

Primer pairs against the big five carbapenemases

A total of five primer pairs were designed against bla_{KPC} and bla_{NDM}, four primer pairs against $bla_{OXA\text{-}48\text{-}like}$, three primer pairs against bla_{VIM} and one primer pair against bla_{IMP} (Table S1‡). The designed primers showed excellent coverage of each of the big five carbapenemase genes. It has been shown that the specificity of RPA is multifactorial. RPA primers with mismatches ($n > 1$) at their 3′ extremity have been shown to inhibit RPA, In addition, 3 mismatches covering both extremities and the centre of the primer sequence negatively affected RPA yield.[26] As such we applied a stringent cut-off limit whereby if a primer displayed >2 mismatches in either the forward or reverse primer to its target gene it was deemed not to provide target sequence coverage. Based on this cut-off, *in silico* analysis of the primers revealed all 46 bla_{KPC} variants were covered as were all 39 bla_{NDM} variants and all 78 bla_{IMP} variants. All 68 bla_{VIM} variants were covered except Vim-7, Vim-61 and Vim-49. All 41 $bla_{OXA\text{-}48\text{-}like}$ genes were covered except Oxa-54. Furthermore Oxa-181 and Oxa-232, frequently produced variants of $bla_{OXA\text{-}48\text{-}like}$ carbapenemases,[27] were found to show 100% identity to the $bla_{OXA\text{-}48\text{-}like}$ targeting primers.

Primer screen

Primer pairs designed against the big five (Table S1‡) were subjected to a RPA primer screen for the purpose of selecting the most sensitive and robust primer pair for each target gene. The nucleotide sequences for $bla_{KPC\text{-}2}$, $bla_{OXA\text{-}48}$, $bla_{NDM\text{-}1}$, $bla_{VIM\text{-}2}$, and $bla_{IMP\text{-}1}$ were each synthesised into individual pUCIDT plasmids and used as the template DNA for RPA reactions. From this point on the $bla_{KPC\text{-}2}$, $bla_{OXA\text{-}48}$, $bla_{NDM\text{-}1}$, $bla_{VIM\text{-}2}$, and $bla_{IMP\text{-}1}$ containing plasmids will be referred to as

KPC, OXA-48, NDM, VIM and IMP, respectively. Each primer pair was empirically evaluated by assessing their activity in duplicate RPA reactions seeded with 90 pM of template DNA specific to the primer pair. No template control (NTC) reactions were set up as negative controls.

All five sets of primers amplified KPC successfully and produced prominent bands near the expected amplicon size of each primer pair (Fig. 1a & b). Each amplicon is migrating at a slightly higher molecular weight than the expected size. This can be attributed to the presence of RPA proteins and crowding agents within the RPA solution forming a DNA–protein-crowding agent complex which migrates slower in gel electrophoresis.[17,28–32] It is recommended by TwistDX that the RPA products should be purified prior to visualising on an agarose gel, however this was avoided to facilitate accurate quantification.[33] Visually, KPC 203 and KPC 114 produced the most amplicon. This observation is supported by densitometry data show in Fig. 1b with a maximum of 402 ng and 292 ng of amplicon produced by KPC 203 and KPC 114, respectively. Faint banding artefacts are observed in the NTC lanes of each primer set. TwistDX protocol's explains that non-specific products are likely to be formed in the NTCs or when using low target copy numbers and can be attributed to primer artefacts.[33] Among the five primer sets, the KPC 203 primer pair demonstrated superior performance in terms of generating the highest quantity of amplicons while exhibiting minimal artefacts in the NTC reaction. Consequently, the KPC 203 primer pair was selected for further RPA assay development.

All primer pairs targeting OXA-48 produced visible amplicons near the expected size (Fig. 1c & d). As noted previously the migration of DNA is retarded slightly by the presence of RPA proteins and crowding agents. The OXA 239 primer pair produced a maximum 343 ng of amplicon, by far the greatest amount of amplicon produced by all the OXA targeting primer pairs (Fig. 1d). Primer pair OXA 194 was the only pair not to produce detectable bands in the NTC; however, a concomitant low quantity of amplicon was produced using these primers. Additionally, high molecular weight bands at ~440 bp and ~500 bp are present when OXA 155 and OXA 186 are used, respectively. These bands are only present when template DNA is added and are not seen in the NTC lanes indicating that the high molecular weight bands may be the product of hairpin-mediated duplication and triplication.[34,35] Therefore, the OXA 239 primer pair was selected for future assay development.

Similar results were obtained using the remaining NDM, VIM and IMP primer sets with NDM 205, Vim 147 and Imp 189 being selected for further analysis (Fig. S2‡).

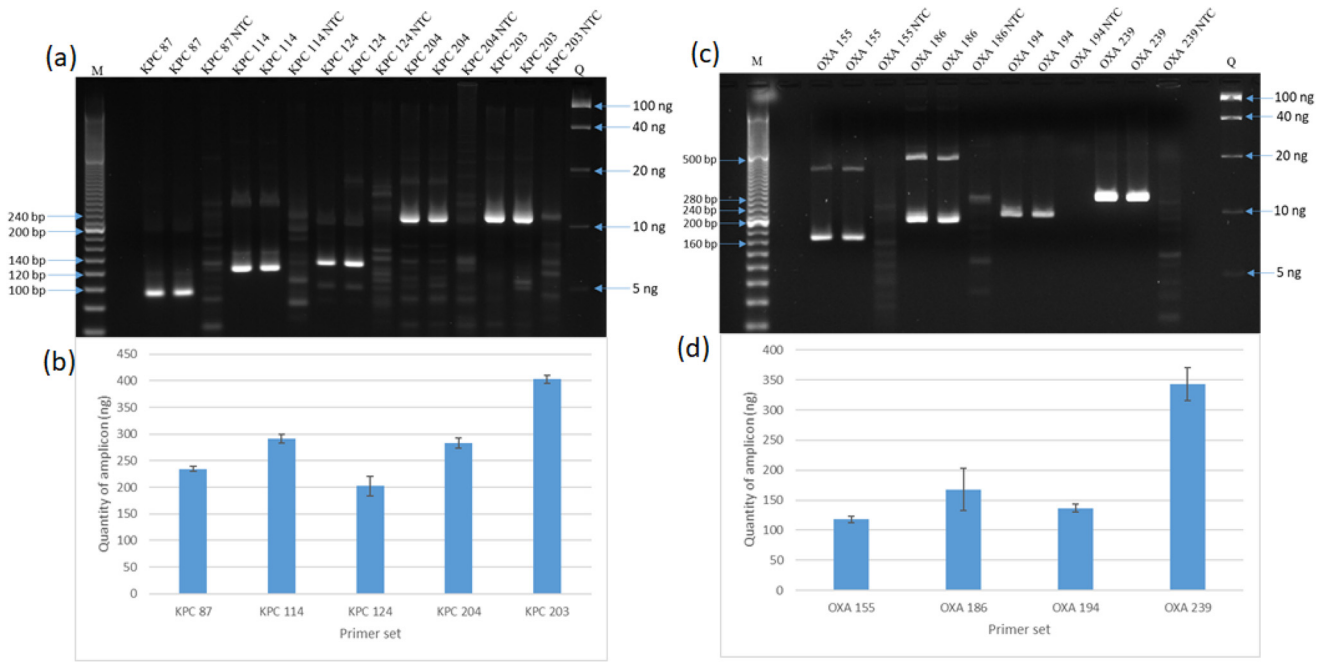

Fig. 1 Agarose gel electrophoresis and densitometry analysis of KPC and OXA primer screens. (a) Agarose gel electrophoresis (3%) of RPA reactions performed at 37 °C for 20 min using five different sets of primers targeted to the KPC gene (KPC 87, KPC 114, KPC 124, KPC 204, KPC 203). RPA reactions were performed in duplicate alongside a single NTC for each primer pair. Lane M – 20 bp molecular weight marker; lane Q – low range quantitation ladder (5–100 ng). (b) Densitometry measuring the quantity of amplicon from an agarose gel electrophoresis loaded with RPA reactions containing 90 pM of KPC template DNA. Error bars represent the range between duplicates. (c) Agarose gel electrophoresis (3%) of RPA reactions performed at 37 °C for 20 min using four different sets of primers targeted to the OXA-48 gene (OXA 155, OXA 186, OXA 194, OXA 239). RPA reactions were performed in duplicate alongside a single NTC for each primer pair. Lane M – 20 bp molecular weight marker; lane Q – low range quantitation ladder (5–100 ng). (d) Densitometry measuring the quantity of amplicon from an agarose gel electrophoresis loaded with RPA reactions containing 90 pM of OXA-48 template DNA. Primer sets are named after the size of the amplicon they produce. Error bars represent the range between duplicates.

Generation of single stranded nucleotide tail sequences

Six unique oligonucleotide tail sequences (Table S2‡), each fifteen nucleotides in length, were designed using an in house bioinformatics script (Fig. S3‡) with the aim of increasing the multiplex capacity.

Solution-phase RPA using tailed forward and reverse primers

Tail number six was allocated as the universal reverse primer tail for the big five (Table S3‡). The remaining five unique tail sequences were allocated to 5′ ends of the forward primers of the big five (Table S3‡). These 5′ tails are the reverse complement of the DNA sequences imparted by their cognate capture probes, and as such, allow capture through a DNA–DNA hybridisation event with the capture probe. Tail allocations were chosen based on minimal secondary structure formation and interaction with other oligonucleotides in the system, as determined by oligoanalyzer (IDT).

Firstly, tailed KPC 203 primers were analysed using solution RPA. Tenfold serial dilutions of KPC template were added to RPA reactions with template starting concentration ranging from 89 pM–8.9 aM. Agarose gel electrophoresis and ELONA were carried out in order to assess the products of the RPA reactions when using these tailed modifications. Visual observations of the agarose gel (Fig. S4a‡) showed the tailed amplicon migrated at a molecular weight ~280 bp. Visible amplicon was generated down to 8.9 fM of starting template. Low molecular weight bands between ~60–100 bp are consistent in each reaction. Notably, these low molecular weight bands are absent from the primer screen (Fig. 1a & c) which used native primers, suggesting it is the presence of the tails which is bringing about their formation. Interestingly, ELONA analysis (Fig. S4b‡) showed no correlation between template concentration and absorbance. As such a sigmoidal curve could not be fitted to this data. High absorbance values in the NTC resulted in a mean absorbance of ~2.05 AU which is higher than most template containing reactions in this assay. The absorbance measured in wells containing buffer only (no RPA components or oligonucleotides) remained low at 0.05 AU which demonstrates that the background is not caused by non-specific binding of the reporter probe or insufficient washing of the RPA reactions post-reporter probe addition. The non-specific signal generated on the ELONA could be caused by primer dimers forming between the forward and reverse primer pairs which each have 5′ single stranded tails exposed to facilitate capture and detection, respectively. This hypothesis is supported by the low molecular weight bands between ~60–100 bp on the agarose gel.

The situations observed for KPC 203 tailed primers was mimicked by the remaining primer pairs OXA 239, NDM 205, VIM 147 and IMP 189. All displayed defined titratable amplicon formation, however, various low molecular weight species were also present (data not shown). Notably these low molecular weight species are more pronounced at RPA reactions which the lowest template DNA concentrations.

To determine whether the low molecular weight species observed in the experiment were primer dimers, additional control reactions were conducted (Fig. S5‡). Consistent with previous experiments, high absorbance values were observed in the NTC wells where both primers and magnesium were present. This finding confirms that the background signal is not caused by the contents of the RPA mastermix. However, negligible absorbance was detected when no primers were included and additionally when RPA was performed without magnesium. This clearly demonstrates that the formation of amplified primer dimers were responsible for the observed background signal.

In summary, the solution-phase RPA strategy using tailed primers produces amplicons of the correct size, as shown by agarose gel electrophoresis (Fig. S4a‡), but in an ELONA readout format false positives hinder the assay (Fig. S4b‡). The investigation in Fig. S5‡ shows that the amplification of primer-dimers, which have both capture and reporter functionalities produce these false positive results. In the absence of the tail sequences the primer pairs produce faint primer artefacts in the NTC reactions (Fig. 1a & c). However, once the tails are present amplified primer dimers can be seen in template containing reactions, especially at low template concentrations, as well as NTC's (Fig. S4a‡). It is these amplified primer dimers which mask the genuine RPA signal imparted by the correct amplicon product through a bringing together of the capture and reporter tails in a primer dimerisation event.

Solid-phase RPA

A solid-phase amplification strategy was designed with the aim of minimising primer dimer formation (Fig. 2). Using this strategy the six unique tails (Fig. S2 & Table S2‡) were then deployed for the modification of the reverse primer (rather than the forward primer as per solution RPA). The tail sequences assigned to each of the primer pairs are shown in Table S4.‡ The use of capture probes is now circumvented by using a 5′ biotin-TEG linker on the forward primers in order to mediate capture at the solid-phase.

Solid-phase assays for each of the big five were carried out as per Experimental section. The assay took a total of 2 h to result including a 40 min RPA amplification time. Shorter amplification times were tested however shorter amplification times resulted in a concomitant increase in LOD (data not shown). Using this 40 min amplification strategy, assays against the big five using unique tails generated calibration curves with *R*-squared values >0.98 (Fig. 3). The LOD's calculated for KPC, OXA, NDM, VIM and IMP were 127.8, 195.7, 20.8, 40.5 and 103.1 fM, respectively. Adopting the solid-phase RPA strategy over solution-phase eliminated the high background absorbance values characteristic of NTC's and samples which contained low amounts of template DNA.

Resonance Raman readout of solid-phase RPA reactions

In an effort to improve the sensitivity and portability of the assay, a portable Raman spectrometer was used to acquire the resonant Raman signal of the electronic transition state of the oxidised TMB substrate. Catalysed oxidation of TMB substrate

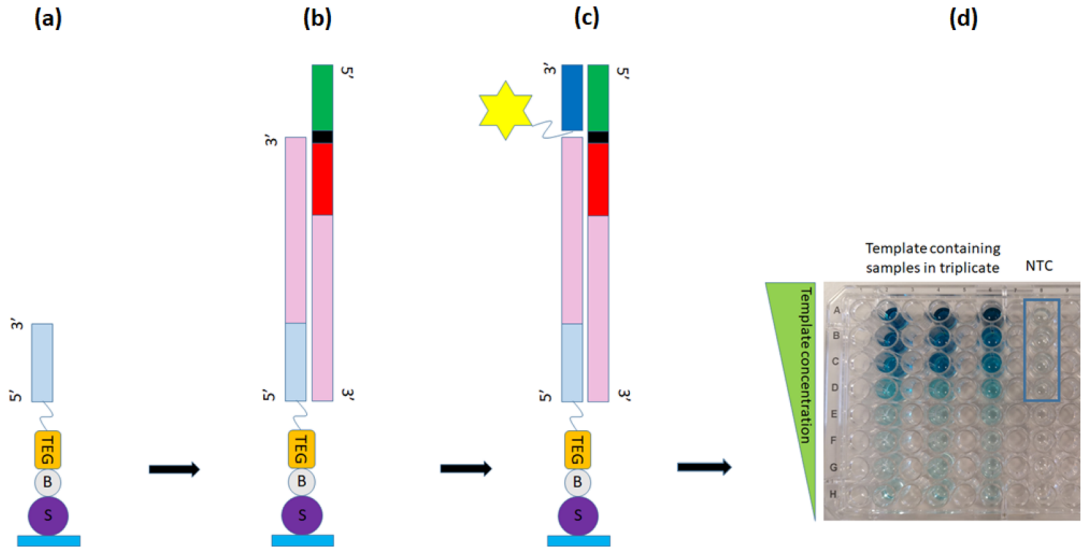

Fig. 2 Schematic representation of solid-phase RPA. (a) Microplate (blue rectangle) coated with streptavidin (purple circle) is functionalised with forward primer (light blue rectangle) specific to its cognate carbapenemase gene using a 5′ biotin-TEG linker (light blue circle and orange rectangle). (b): If the target gene is present the amplicon (pink rectangle) extends and incorporates a 5′ tail (green rectangle) mediated by a reverse primer (red rectangle) containing a C3 blocker (black rectangle). (c): A reporter probe (dark blue rectangle) containing a 5′ horseradish perdoxidase (HRP) modification (yellow star) bind to the 5′ tail *via* a DNA–DNA hybridisation. (d): The HRP turns TMB substrate blue and the absorbance is measured on a benchtop platereader @ 630 nm. NTC = no template control.

yields multiple oxidised states. The first step in the oxidation yields a radical cation in equilibrium with a charge transfer complex (CTC), it is this CTC molecule that elicits the blue colour change. The proposed target compound within our study is the CTC oxidised form of TMB which has an electronic transition with a λ_{max} of 650 nm.[36]

Within this study the group excited the CTC using a laser excitation wavelength of 633 nm and measured the intensity of the Raman spectral band at 1611 cm^{-1} which is unique to the CTC.[37] Accordingly, in our study the laser wavelength was tuned to be in resonance with the oxidised TMB, thus resulting in enhancement of the Raman bands at 1611, 1339 and 1193 cm^{-1} (Fig. S6‡) which was in agreement with previous studies.[24,38]

Solid-phase RPA assay calibration curves were carried out against the big five, however rather than measuring absorbance at 630 nm using a benchtop microplate reader, reactions were analysed using the intensity of the Raman band at 1611 cm^{-1} using a 638 nm portable Raman spectrometer. Calibration curves for the big five are shown in Fig. 3. When comparing the LOD derived using a absorbance based plate reader compared to the portable Raman spectrometer there is an improvement of between a 1.2–19.7 fold in the LOD when using the portable Raman reader (Table 1). While each reporter probe contains an identical HRP molecule, it is tethered to the RPA amplicon through a unique DNA sequence. This presumably leads to subtle differences in HRP presentation between targets, causing variations in the resulting CTC. The varying degrees of improvement are likely attributed to the unique properties of each target, affecting the characteristics of the CTC and Raman signal detection. It is important to note the overall trend is consistent across the two readouts and ten assays and whilst some variation in the degrees of difference is observed, the data taken as a whole demonstrates a robust set of assays.

Towards a point-of-care solid-phase RPA assay

The fact that the portable Raman reader linked to RRS detection results in an improved LOD over a classical laboratory benchtop microplate spectrophotometer bodes well for a remote PoC solution in the future. Our approach would not replace existing protocols that uncover carbapenem hydrolysis,[39] but has the potential to be a rapid portable method with a role in outbreak control, monitoring resistance gene dissemination and potentially advising clinicians of which drug inhibitor combinations would be advantageous for the patient on a ward setting.

Carbapenemase genes are typically screened in various clinical samples to detect the presence of CPO. The choice of samples depends on the suspected infection site, the patient's clinical condition, and the type of healthcare setting. RPA has exhibited a specific resistance to prevalent PCR inhibitors, and its functionality has been demonstrated with nucleic acids obtained from diverse sample sources with minimal sample pre-treatment. These include, but are not limited to, blood, serum, nasal and vaginal swabs, plasma, stool, and urine.[14] However, there are specific examples where components involved in the sample preparation such as the DNA extraction buffer or bacterial growth medium have been shown to inhibit the RPA reaction.[40,41] Consequently, there is a need for empirical assessment to ascertain how the specific clinical sample and its pre-treatment impact the efficiency of the RPA assay.

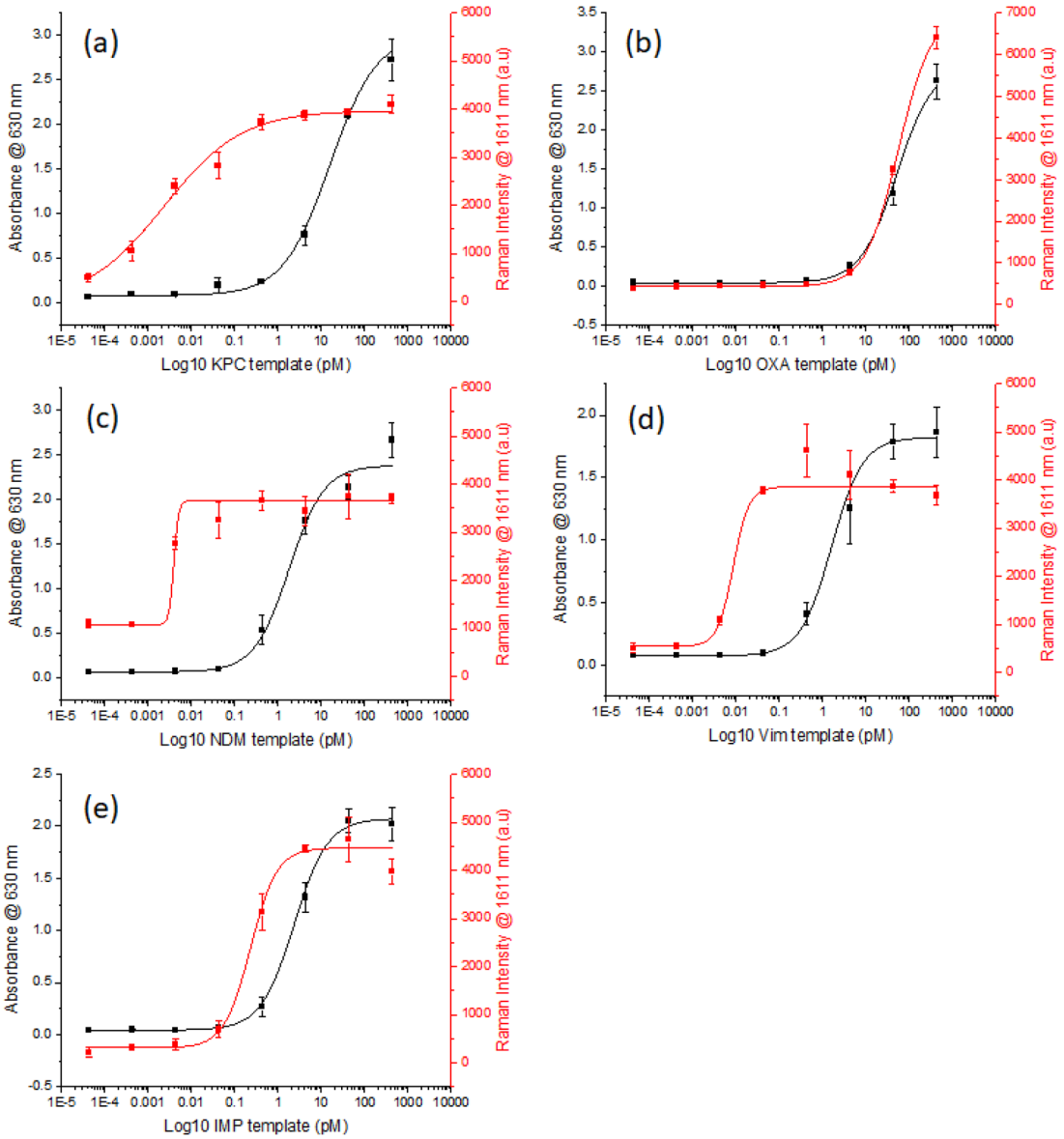

Fig. 3 Solid-phase RPA calibration curves generated against the big 5 carbapenemase genes using a benchtop microplate reader or a portable Raman spectrometer. Microplate wells were seeded with a template DNA from either (a) KPC, (b) OXA, (c) NDM, (d) VIM or (e) IMP and subjected to solid-phase RPA and ELONA analysis before curves were read using a benchtop microplate reader (black line) or a portable Raman spectrometer (red line). *R*-Squared values for all curves are >0.98. All curves were fitted to a logistic sigmoidal fitting function (Origin 2020).

Table 1 LOD comparison of the big 5 detected using a benchtop platereader *vs.* a portable Raman spectrometer

	LOD (fM)		
Gene	Platereader (A)	Portable Raman spectrometer (B)	Fold increase (A/B)
KPC	127.8	6.5	19.7
VIM	40.5	4.1	9.9
NDM	20.8	3.8	5.5
IMP	103.1	31.6	3.3
OXA-48	195.7	156.9	1.2

This empirical evaluation is crucial for ensuring accurate and reliable results tailored to the unique characteristics of each clinical sample. The team will carry out a clinical evaluation once the solid-phase assay has been transferred to magnetic beads and a microfluidic cartridge – see Conclusions for more details.

The solid-phase assay developed in this work has no background primer dimer artefacts allowing fM LOD's to be quantified for each gene, namely, 6.5 fM, 156.9 fM, 3.8 fM, 4.1 fM and 31.6 fM for KPC, OXA, NDM, VIM and IMP respectively. Expressed as copies per μL the solid-phase assays employing a portable Raman spectrometer have LOD's in DNA copy number per μL of 3.87×10^4, 9.29×10^4, 2.25×10^3, 2.44×10^3

and 1.87×10^4 for KPC, OXA, NDM, VIM and IMP, respectively. A lower LOD would normally be expected in a solution based systems due to the unimpeded diffusion of primers/reaction reagents providing favourable amplification kinetics and hence lower LOD.[16] However, in our assay design the solution-phase RPA background signal shown in Fig. S4‡ exemplifies why Piepenburg *et al.* opted for a primer/probe system that negates any primer dimer background signal when using fluorescent readout on a benchtop instrument.[18] Significantly, our work demonstrates that even though solid-phase RPA will have slightly lower amplification kinetics, it remains capable of achieving a remarkably competitive LOD using a portable RRS reader. Moreover, the development of a carbapenemase RPA assay that relies solely on oligonucleotide tails for hybridisation and employs a single enzyme tag for readout is a considerable simplification in complexity compared to previous assay designs. For example, RPA NALFIA (nucleic acid lateral flow immunoassay) approaches discussed in the literature require multiple antibodies and probes to generate lateral flow sandwich immunoassays.[42,43]

Conclusions

In this study, we successfully identified the big five carbapenemase genes using a spatially separated solid-phase RPA assay conducted on a streptavidin-coated microplate. Detection was accomplished using both a benchtop microplate reader and a portable Raman spectrometer, resulting in a substantial enhancement of signals with low fM LOD's. While the current assay operates in a laboratory setting, employing a streptavidin-coated microplate as the solid-phase, we have demonstrated the potential for miniaturisation of the reader. Additionally, future adaptation of the solid-phase approach to streptavidin-coated magnetic beads would facilitate the translation of the assay into a microfluidic cartridge, reaching higher technology readiness levels (3–6).

Bead-based amplification strategies have gained prominence in molecular diagnostic applications, particularly in infectious disease detection.[44] These strategies employ microbeads coated with specific probes or primers for detecting and quantifying target nucleic acid sequences. They offer advantages such as multiplex capacity, high sensitivity and selectivity, ease of use and automation, flexibility, and stability.[45] Future research directions include coupling a magnetic bead amplification strategy with a surface-enhanced Raman scattering readout. This advancement would enable ultrasensitive detection, spectral deconvolution, and quantification of each of the big five carbapenemases in a PoC single-tube multiplex assay.

Conflicts of interest

There are no conflicts of interest to declare.

Acknowledgements

EP/K031953/1 EPSRC IRC in Early-Warning Sensing Systems for Infectious Diseases.

EP/R00529X/1 i-sense: EPSRC IRC in Agile Early Warning Sensing Systems for Infectious Diseases and Antimicrobial Resistance.

EP/R018391/1 IRC Next Steps Plus: Ultra-Sensitive Enhanced NanoSensing of Anti-Microbial Resistance (u-Sense).

References

1 T. R. Walsh, Emerging carbapenemases: a global perspective, *Int. J. Antimicrob. Agents*, 2010, **36**, S8–S14.
2 S. Pournaras, R. Zarrilli, P. G. Higgins and C. Tsioutis, Carbapenemase-Producing Organisms as Leading Cause of Hospital Infections, *Front. Med.*, 2021, 1924.
3 F. S. Codjoe and E. S. Donkor, Carbapenem resistance: a review, *Med. Sci.*, 2017, **6**(1), 1.
4 G. Meletis, Carbapenem resistance: overview of the problem and future perspectives, *Ther. Adv. Infect. Dis.*, 2016, **3**(1), 15–21.
5 R. A. Bonomo, E. M. Burd, J. Conly, B. M. Limbago, L. Poirel, J. A. Segre, *et al.*, Carbapenemase-producing organisms: a global scourge, *Clin. Infect. Dis.*, 2018, **66**(8), 1290–1297.
6 Y.-L. Lee, H.-M. Chen, M. Hii and P.-R. Hsueh, Carbapenemase-producing Enterobacterales infections: Recent advances in diagnosis and treatment, *Int. J. Antimicrob. Agents*, 2022, 106528.
7 R. P. Ambler, The structure of beta-lactamases, *Philos. Trans. R. Soc. London, Ser. B*, 1980, **289**(1036), 321–331.
8 V. G. Vandavasi, P. S. Langan, K. L. Weiss, J. M. Parks, J. B. Cooper, S. L. Ginell, *et al.*, Active-Site Protonation States in an Acyl-Enzyme Intermediate of a Class A β-Lactamase with a Monobactam Substrate, *Antimicrob. Agents Chemother.*, 2017, **61**(1), e01636–e01616.
9 H. Feng, X. Liu, S. Wang, J. Fleming, D.-C. Wang and W. Liu, The mechanism of NDM-1-catalyzed carbapenem hydrolysis is distinct from that of penicillin or cephalosporin hydrolysis, *Nat. Commun.*, 2017, **8**(1), 2242.
10 M. Tato, P. Ruiz-Garbajosa, M. Traczewski, A. Dodgson, A. McEwan, R. Humphries, *et al.*, Multisite Evaluation of Cepheid Xpert Carba-R Assay for Detection of Carbapenemase-Producing Organisms in Rectal Swabs, *J. Clin. Microbiol.*, 2016, **54**(7), 1814–1819.
11 F. C. Tenover, R. Canton, J. Kop, R. Chan, J. Ryan, F. Weir, *et al.*, Detection of Colonization by Carbapenemase-Producing Gram-negative Bacilli in Patients by Use of the Xpert MDRO Assay, *J. Clin. Microbiol.*, 2013, **51**(11), 3780–3787.
12 I. Y. Yoo, D. P. Shin, W. Heo, S. I. Ha, Y. J. Cha and Y.-J. Park, Comparison of BD MAX Check-Points CPO assay with Cepheid Xpert Carba-R assay for the detection of carbapenemase-producing Enterobacteriaceae directly from

rectal swabs, *Diagn. Microbiol. Infect. Dis.*, 2022, **103**(3), 115716.
13 R. H. Liu, J. Yang, R. Lenigk, J. Bonanno and P. Grodzinski, Self-contained, fully integrated biochip for sample preparation, polymerase chain reaction amplification, and DNA microarray detection, *Anal. Chem.*, 2004, **76**(7), 1824–1831.
14 R. K. Daher, G. Stewart, M. Boissinot and M. G. Bergeron, Recombinase polymerase amplification for diagnostic applications, *Clin. Chem.*, 2016, **62**(7), 947–958.
15 Z. A. Crannell, B. Rohrman and R. Richards-Kortum, Equipment-free incubation of recombinase polymerase amplification reactions using body heat, *PLoS One*, 2014, **9**(11), e112146.
16 I. M. Lobato and C. K. O'Sullivan, Recombinase polymerase amplification: Basics, applications and recent advances, *TrAC, Trends Anal. Chem.*, 2018, **98**, 19–35.
17 J. Li, J. Macdonald and F. von Stetten, Review: a comprehensive summary of a decade development of the recombinase polymerase amplification, *Analyst*, 2019, **144**(1), 31–67.
18 O. Piepenburg, C. H. Williams, D. L. Stemple and N. A. Armes, DNA detection using recombination proteins, *PLoS Biol.*, 2006, **4**(7), e204.
19 TwistDx. TwistAmp® DNA amplification kits', Combined instruction manual, 2016.
20 J. S. del Río, N. Y. Adly, J. L. Acero-Sánchez, O. Y. Henry and C. K. O'Sullivan, Electrochemical detection of Francisella tularensis genomic DNA using solid-phase recombinase polymerase amplification, *Biosens. Bioelectron.*, 2014, **54**, 674–678.
21 A. M. Ichzan, S.-H. Hwang, H. Cho, C. San Fang, S. Park, G. Kim, *et al.*, Solid-phase recombinase polymerase amplification using an extremely low concentration of a solution primer for sensitive electrochemical detection of hepatitis B viral DNA, *Biosens. Bioelectron.*, 2021, **179**, 113065.
22 J. S. Del Río, I. M. Lobato, O. Mayboroda, I. Katakis and C. K. O'Sullivan, Enhanced solid-phase recombinase polymerase amplification and electrochemical detection, *Anal. Bioanal. Chem.*, 2017, **409**, 3261–3269.
23 E. Smith and G. Dent, *Modern Raman spectroscopy: a practical approach*, John Wiley & Sons, 2019.
24 L. Jensen, L. Zhao, J. Autschbach and G. Schatz, Theory and method for calculating resonance Raman scattering from resonance polarizability derivatives, *J. Chem. Phys.*, 2005, **123**(17), 174110.
25 W. Hassanain, C. Johnson, K. Faulds, D. Graham and N. Keegan, Recent advances in antibiotic resistance diagnosis using SERS: focus on the "Big 5" challenges, *Analyst*, 2022, **147**(21), 4674–4700.
26 R. K. Daher, G. Stewart, M. Boissinot, D. K. Boudreau and M. G. Bergeron, Influence of sequence mismatches on the specificity of recombinase polymerase amplification technology, *Mol. Cell. Probes*, 2015, **29**(2), 116–121.
27 C. Shankar, P. Mathur, M. Venkatesan, A. K. Pragasam, S. Anandan, S. Khurana, *et al.*, Rapidly disseminating bla OXA-232 carrying Klebsiella pneumoniae belonging to ST231 in India: multiple and varied mobile genetic elements, *BMC Microbiol.*, 2019, **19**, 1–8.
28 M. A. Londoño, C. L. Harmon and J. E. Polston, Evaluation of recombinase polymerase amplification for detection of begomoviruses by plant diagnostic clinics, *Virol J.*, 2016, **13**, 48.
29 S. Kersting, V. Rausch, F. F. Bier and M. von Nickisch-Rosenegk, Multiplex isothermal solid-phase recombinase polymerase amplification for the specific and fast DNA-based detection of three bacterial pathogens, *Mikrochim. Acta*, 2014, **181**(13–14), 1715–1723.
30 L. Glais and E. Jacquot, Detection and Characterization of Viral Species/Subspecies Using Isothermal Recombinase Polymerase Amplification (RPA) Assays, in *Plant Pathology: Techniques and Protocols*, ed. C. Lacomme, Springer New York, New York, NY, 2015, pp. 207–225.
31 B. Babu, B. K. Washburn, S. H. Miller, K. Poduch, T. Sarigul, G. W. Knox, *et al.*, A rapid assay for detection of Rose rosette virus using reverse transcription-recombinase polymerase amplification using multiple gene targets, *J. Virol. Methods*, 2017, **240**, 78–84.
32 Q. Liu, B. K. L. Lim, S. Y. Lim, W. Y. Tang, Z. Gu, J. Chung, *et al.*, Label-free, real-time and multiplex detection of Mycobacterium tuberculosis based on silicon photonic microring sensors and asymmetric isothermal amplification technique (SPMS-AIA), *Sens. Actuators, B*, 2018, **255**, 1595–1603.
33 TwistDx. TwistAmp® DNA amplification kits COMBINED INSTRUCTION MANUAL., (2014), 16, 7.
34 O. Piepenburg, C. H. Williams, D. L. Stemple and N. A. Armes, DNA detection using recombination proteins, *PLoS Biol.*, 2006, **4**(7), e204.
35 A. Salazar, F. M. Ochoa-Corona, J. L. Talley and B. H. Noden, Recombinase polymerase amplification (RPA) with lateral flow detection for three Anaplasma species of importance to livestock health, *Sci. Rep.*, 2021, **11**(1), 15962.
36 S. Laing, K. Gracie and K. Faulds, Multiplex in vitro detection using SERS, *Chem. Soc. Rev.*, 2016, **45**(7), 1901–1918.
37 S. Laing, A. Hernandez-Santana, J. Sassmannshausen, D. L. Asquith, I. B. McInnes, K. Faulds, *et al.*, Quantitative Detection of Human Tumor Necrosis Factor α by a Resonance Raman Enzyme-Linked Immunosorbent Assay, *Anal. Chem.*, 2011, **83**(1), 297–302.
38 L. Zhan, S. J. Zhen, X. Y. Wan, P. F. Gao and C. Z. Huang, A sensitive surface-enhanced Raman scattering enzyme-catalyzed immunoassay of respiratory syncytial virus, *Talanta*, 2016, **148**, 308–312.
39 P. Nordmann, L. Poirel and L. Dortet, Rapid detection of carbapenemase-producing Enterobacteriaceae, *Emerging Infect. Dis.*, 2012, **18**(9), 1503.
40 N. Valasevich and B. Schneider, Rapid detection of "Candidatus Phytoplasma mali" by recombinase polymerase amplification assays, *J. Phytopathol.*, 2017, **165**(11–12), 762–770.
41 H.-B. Liu, Y.-X. Zang, X.-J. Du, P. Li and S. Wang, Development of an isothermal amplification-based assay

for the rapid visual detection of Salmonella bacteria, *J. Dairy Sci.*, 2017, **100**(9), 7016–7025.

42 B. Jin, B. Ma, J. Li, Y. Hong and M. Zhang, Simultaneous detection of five foodborne pathogens using a mini automatic nucleic acid extractor combined with recombinase polymerase amplification and lateral flow immunoassay, *Microorganisms*, 2022, **10**(7), 1352.

43 F. Wang, L. Wang, H. Chen, N. Li, Y. Wang, Y. Li, *et al.*, Rapid detection of blaKPC, blaNDM, blaOXA-48-like and blaIMP carbapenemases in Enterobacterales using recombinase polymerase amplification combined with lateral flow strip, *Front. Cell. Infect. Microbiol.*, 2021, **11**, 1223.

44 S. Carinelli, M. Marti, S. Alegret and M. I. Pividori, Biomarker detection of global infectious diseases based on magnetic particles, *New Biotechnol.*, 2015, **32**(5), 521–532.

45 C. Tang, Z. He, H. Liu, Y. Xu, H. Huang, G. Yang, *et al.*, Application of magnetic nanoparticles in nucleic acid detection, *J. Nanobiotechnol.*, 2020, **18**(1), 1–19.